processes

MDPI

Article

Reaction Kinetics of Carbon Dioxide in Aqueous Blends of N-Methyldiethanolamine and L-Arginine Using the Stopped-Flow Technique

Nafis Mahmud [1], Abdelbaki Benamor [1,*], Mustafa Nasser [1], Muftah H. El-Naas [1] and Paitoon Tontiwachwuthikul [2]

[1] Gas Processing Centre, College of Engineering, Qatar University, Doha 2713, Qatar; n.mahmud@qu.edu.qa (N.M.); m.nasser@qu.edu.qa (M.N.); muftah@qu.edu.qa (M.H.E.-N.)

[2] Clean Energy Technology Research Institute (CETRI), Faculty of Engineering, University of Regina, 3737 Wascana Parkway, Regina, SK S4S 0A2, Canada; paitoon@uregina.ca

* Correspondence: benamor.abdelbaki@qu.edu.qa; Tel.: +974-4403-4381; Fax: +974-4403-4371

Received: 7 January 2019; Accepted: 29 January 2019; Published: 6 February 2019

Abstract: Reduction of carbon dioxide emission from natural and industrial flue gases is paramount to help mitigate its effect on global warming. Efforts are continuously deployed worldwide to develop efficient technologies for CO_2 capture. The use of environment friendly amino acids as rate promoters in the present amine systems has attracted the attention of many researchers recently. In this work, the reaction kinetics of carbon dioxide with blends of N-methyldiethanolamine and L-Arginine was investigated using stopped flow technique. The experiments were performed over a temperature range of 293 to 313 K and solution concentration up to one molar of different amino acid/amine ratios. The overall reaction rate constant (k_{ov}) was found to increase with increasing temperature and amine concentration as well as with increased proportion of L-Arginine concentration in the mixture. The experimental data were fitted to the zwitterion and termolecular mechanisms using a nonlinear regression technique with an average absolute deviation (AAD) of 7.6% and 8.0%, respectively. A comparative study of the promoting effect of L-Arginine with that of the effect of Glycine and DEA in MDEA blends showed that MDEA-Arginine blend exhibits faster reaction rate with CO_2 with respect to MDEA-DEA blend, while the case was converse when compared to the MDEA-Glycine blend.

Keywords: Reaction; kinetics; carbon dioxide; N-methyldiethanolamine; L-Arginine; stopped flow technique

1. Introduction

The rapid growth of world economies associated with increased fossil fuel consumption for energy needs resulted in the generation of large amounts of greenhouse gases accumulated in the atmosphere. Carbon dioxide (CO_2) is a major contributor to greenhouse gases accountable to the observed climate change and associated environmental problems. Reducing CO_2 concentration in the atmosphere to an acceptable level is necessary for future generation's well-being. Different options are available to capture CO_2; however, amine based reactive solvents is one of the most mature and successful technology used in the industry, especially from large point sources, such as natural gas treatment units and power generation plants [1–6]. Large variants of amine based solvents are available in the market, many of which contain proprietary additives to enhance their absorption performances. Amine based solvents are known by their high absorption capacities and their ability to selectively absorb CO_2/H_2S from natural and flue gases. Conventional amine solvents, such as primary monoethanolamine (MEA), 2-amino-2-methyl-1-propanol (AMP), secondary

diethanolamine (DEA), tertiary amine N-methyldiethanolamine (MDEA) and polyamines (such as piperazine (PZ), 2-(2-aminoethylamino) ethanol (AEEA) are efficient for capturing CO_2 from various industrial processes and are still the choice in the industry because of the well-known absorption-regeneration process. However, several drawbacks like low absorption rate, periodic solvent make up to compensate for solvent losses, high regeneration energy requirement and severe equipment corrosion are still associated with their use [7–11].

Liquid tertiary amines, such as MDEA have higher theoretical sorption capacity with a ratio of 1:1 mol [12] but the reaction rate is much slower. To overcome this drawback, blended amines have been suggested [7]. To take advantage of their high loading capacity, low degradation rate and low energy for regeneration, tertiary amines are mixed with faster reacting primary/secondary amines or piperazine to develop new solvents with better CO_2 capture performance such as high absorption and cyclic capacity, fast reaction kinetics, low corrosion, degradation and less heat duty requirement [13,14].

Amino acids, usually called alkaline salts of amines, have recently drawn attention to CO_2 capture due to their exceptional properties [15]. The structure of amino acids consists of two important functional groups, namely amine (-NH_2) and carboxylic acid (-COOH) or a sulfonic acid group [16]. Their salt nature makes their volatilities negligible which results in low solvent losses [17]. Their low environmental impact and high biodegradability [18] make them more environmentally friendly [19]. In addition, amino acids have high resistance to oxidative degradation making them a right choice for CO_2 capture from flue gases containing large amounts of oxygen [20]. However, at high concentration or at high CO_2 loading, they tend to precipitate resulting in lower mass transfer [21], which is a major drawback.

Nevertheless, several studies has reported on CO_2 capture using amino acids [22–25]. Siemens developed an amino acid based process and claim it has a reduced energy consumption of about 73% compared to the conventional MEA process [26]. Aqueous solutions of sodium glycinate were proposed for CO_2 absorption [27,28]. Shen et al. [29,30] used potassium salts of lysine and Histidine for CO_2 absorption and concluded that histidine reactivity towards CO_2 was comparable to that of MEA. Portugal et al. [31] used potassium glycinate and potassium threonate for CO_2 absorption purposes [32]. Huang et al. [33] and Wei et al. [34] determined the reaction rate constant of taurate carbamate formation during the absorption of CO_2 into CO_2-free and CO_2-loaded taurate solutions using a wetted-wall column at a temperature range of 293–353 K. The properties necessary for mass transfer evaluation, such us density, viscosity, CO_2 diffusivity, N_2O solubility were reported for several amino acids under different conditions [35–40].

In a previous study on reaction kinetics of amino acids with CO_2, it was observed, that L-Arginine, an amino acid, showed faster reaction rate compared to that of Glycine and Sarcosine when used as a single solvent [41]. Another study on the promoting effect of Glycine in MDEA blends showed that the reaction rate of MDEA with CO_2 could be significantly increased by the presence of an amino acid promoter [42]. However, the promoting effect of L-Arginine in MDEA blends remain unknown. In this work, the reaction kinetics of CO_2 with aqueous mixtures of MDEA and L-Arginine were determined using the stopped flow technique. The temperature was varied from 298 to 313 K and the amine total concentration was varied from 0.25 to 1 mol of different proportions of Arg/MDEA. Our findings provide a new insight to the use of Arg as rate promoter for CO_2 capture blended tertiary amines. The molecular structure of MDEA and L-Arginine are shown in the Figure 1.

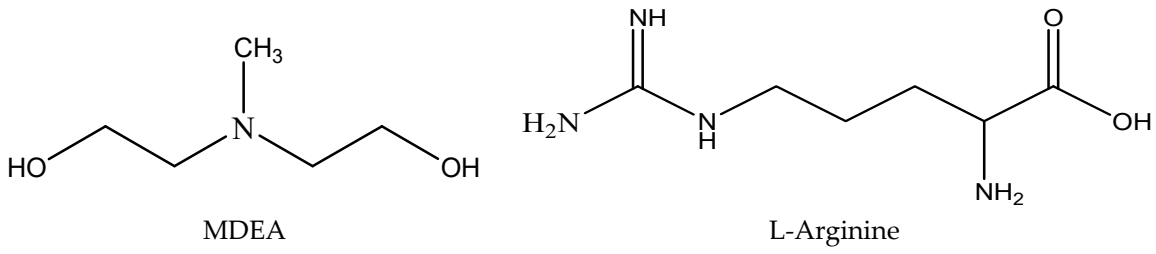

Figure 1. Molecular Structure of MDEA (N-methyldiethanolamine) and L-Arginine.

2. Reaction Models

2.1. Reaction of CO_2 with MDEA

It is widely accepted that the reactions of CO_2 with primary amines results in formation of a carbamate and a bicarbonate products. However, in case of tertiary amines, only bicarbonates are formed during the reaction with CO_2. Therefore, MDEA being a tertiary amine will also not form any carbamates and their reaction of CO_2 in aqueous solution is as follows [21]:

$$CO_2 - H_3CN(C_2H_4OH)_2 + H_2O \xrightarrow{k_{MDEA}} H_3CNH^+(C_2H_4OH)_2 + HCO_3^- \quad (1)$$

Its pseudo-first-order reaction rate is:

$$r_{CO_2-MDEA} = -k_{MDEA}[CO_2][MDEA] \quad (2)$$

In addition to this reaction, the formation of bicarbonates in aqueous systems may be considered:

$$CO_2 + OH^- \xrightarrow{k_{OH}} HCO_3^- \quad (3)$$

Its rate of reaction was given as [43]:

$$r_{CO_2-OH} = -k_{OH}[CO_2][OH^-] \quad (4)$$

2.2. Reaction of CO_2 with Amino Acid

2.2.1. Zwitterion Mechanism

This mechanism was first coined by Caplow to comprehend the reactions of primary or secondary amines with CO_2 [44]. Amino acid [$NHR_1R_2COO^-$] has a molecular structure similar to that of primary or secondary amines. Its reaction pathway with CO_2 is considered to be similar to that of CO_2-amines and usually yields the formation of carbamate ion through two successive steps: (i) the formation of an intermediate zwitterion according to Reaction 5, (ii) proton removal by any base present in the solution according to Reaction 6 [22].

$$CO_2 + NHR_1R_2COO^- \underset{k_{-1}}{\overset{k_1}{\rightleftharpoons}} {}^-OOCN^+R_1R_1COO^- \quad (5)$$

$${}^-OOCNH^+R_1R_2COO^- + B_i \xrightarrow{k_{b,i}} {}^-OOCNR_1R_2COO^- + BH^+ \quad (6)$$

The corresponding reaction rate is given as [20]:

$$r_{CO2-Arg} = -k_2[Arg][CO_2] \Big/ \left(1 + \left(k_{-1} \Big/ \left(\sum_i k_{b_i}[B_i]\right)\right)\right) \quad (7)$$

where the term 'k_{bi}' represents the deprotonation rate constant of the zwitterion by any base. The reaction rate constant can be written as:

$$k_{Arg} = -k_2[Arg] \Big/ \left(1 + \left(k_{-1} \Big/ \left(\sum_i k_{b_i}[B_i]\right)\right)\right) \quad (8)$$

The analysis of this model reveals two asymptotic cases, namely, $1 >> \frac{k_{-1}}{\sum_i k_{b_i}[B_i]}$ and $1 << \frac{k_{-1}}{\sum_i k_{b_i}[B_i]}$. When the formation of the zwitterion carbamate following Reaction 5 is the rate-limiting step. The first case prevails, thus, Equation (7) reduces to:

$$k_{Arg} = -k_2[Arg] \tag{9}$$

In the opposite case, when $1 << \frac{k_{-1}}{\sum_i k_{b_i}[B_i]}$, the proton removal from the zwitterion intermediate according to Reaction 6 is the rate limiting step; Equation (7) then becomes:

$$k_{Arg} = -k_2[Arg]\left(\sum_i k_{b_i}[B_i]\right) \Big/ k_{-1} \tag{10}$$

In the latter case, the reaction order dependency on the amino acid concentration varies from one to two. This phenomenon is commonly observed in CO_2 reaction with primary and secondary amines [26,27] and was proved to prevail in other salts of amino acids [28].

2.2.2. Termolecular Mechanism

Crooks and Donnellan [45] proposed an alternative single-step termolecular mechanism, which involves only one-step in the reaction process as shown in the Figure 2 below.

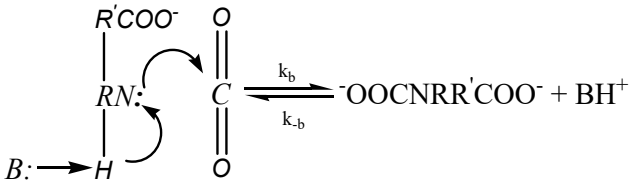

Figure 2. Termolecular Mechanism.

This mechanism was further investigated by Silva and Svendson [46], based on which they suggested that the reaction progresses through the bonding of the CO_2 molecule with the amine, which is stabilized by solvent molecules with hydrogen bonds. This in turn results in the formation of loosely bounded complex. They also added that the carbamate will be formed only when the amine molecule is in the vicinity of zwitterion. An analysis of the rate expression of the termolecular mechanism shows that the reaction of CO_2 with amine is second order with respect to amine. Therefore, in this case, Equation (7) becomes:

$$r_{CO_2} = k_{ov}[CO_2] = [CO_2][Arg]\left\{\sum k_{b_i}[B_i]\right\} \tag{11}$$

Regardless of the mechanism employed, a carbamate and a protonated base are the generally accepted products of the CO_2 reaction with amine.

2.3. Reaction of CO_2 with Mixtures of MDEA and L-Arginine

For blends of MDEA and L-Arginine, the overall reaction rate with CO_2 is considered as the sum of reaction rates of CO_2-MDEA and CO_2-L-Arginine, hence:

$$r_{CO_2} = r_{CO_2-Arg} + r_{CO_2-MDEA} + r_{CO_2-OH} \tag{12}$$

which can be written as:

$$r_{CO_2} = -\left(k_2[Arg] \Big/ \left(1 + \left(k_{-1} / \sum_i k_{b_i}[B_i]\right)\right) + k_{MDEA}[MDEA]\right)[CO_2] \tag{13}$$

or

$$r_{CO_2} = \left(k_{Arg} + k_{MDEA}[MDEA]\right)[CO_2] = k_{ov}[CO_2] \tag{14}$$

In case of aqueous solution of L-Arginine, water molecules, 'H_2O'; hydroxyl ions, 'OH-' and deprotonated amino acid, 'L-Arginine', act as bases. Therefore, if the reaction is expected to proceed via the zwitterion mechanism, then the based on Equation (8), the term 'k_{Arg}' can be defined as follows:

$$k_{Arg} = -\frac{k_2[Arg]}{1+\left(k_{-1}/\left(k'_{Arg}[Arg]+k'_{OH^-}[OH^-]+k'_{MDEA}[MDEA]+k'_{H_2O}[H_2O]\right)\right)} \quad (15)$$

which can be written as:

$$k_{Arg} = -\frac{[Arg]}{\frac{1}{k_2}+\left(1/\left(\frac{k_2k'_{Arg}}{k_{-1}}[Arg]+\frac{k_2k'_{OH^-}}{k_{-1}}[OH^-]+\frac{k_2k'_{MDEA}}{k_{-1}}[MDEA]+\frac{k_2k'_{H_2O}}{k_{-1}}[H_2O]\right)\right)} \quad (16)$$

By defining new constants, k_a, k_{hyd}, k_b and k_w as $k_a = \frac{k_2\, k\,'_{Arg}}{k_{-1}}$, $k_{hyd} = \frac{k_2\, k\,'_{OH}}{k_{-1}}$, $k_b = \frac{k_2\, k\,'_{MDEA}}{k_{-1}}$ and $k_w = \frac{k_2k'_{H_2O}}{k_{-1}}$. Equation (13) becomes:

$$k_{Arg} = \frac{[Arg]}{(1/k_2)+\left(1/\left(k_a[Arg]+k_{hyd}[OH^-]+k_b[MDEA]+k_w[H_2O]\right)\right)} \quad (17)$$

However, if the reaction is expected to proceed via the termolecular mechanism, the term, 'k_{Arg}' can be redefined as follows:

$$k_{Arg} = [Arg]\left\{k_a[Arg]+k_w[H_2O]+k_{hyd}[OH^-]\right\} \quad (18)$$

3. Materials and Methods

3.1. Materials

Reagents used in this work were analytical grade N-methyldiethanolamine (MDEA) with a mass purity of 99% obtained from Sigma-Aldrich and L-Arginine with purity of 99% purchased from Fluka (St. Louis, MS, USA). All chemicals were used as received without further purification. CO_2 solutions were prepared by bubbling analytical grade CO_2 (99.99%) for at least half an hour in deionised water. Deionised water was used as solvent throughout the experiments.

3.2. Methods

Pseudo first-order kinetics of CO_2 reaction with different aqueous mixtures of L-Arginine in MDEA were measured using stopped-flow apparatus (Hi-Tech Scientific Ltd., and Model SF-61DX2, Bradford-on-Avon, Wiltshire, UK) with a dead time of 1 ms. The apparatus essentially consists of working syringes immersed in water bath, where the reacting solutions are loaded. It also contains a pneumatically controlled drive plate to load the reacting solutions into a mixer and the conductivity of the mixed solution is measured within the conductivity cell. Finally, the mixed solution is collected in a stopping syringe. A schematic diagram of the Stopped-Flow Apparatus has been presented in Figure 3 below.

An external water bath (Alpha RA8, Lauda, Delran, NJ, USA) was used to control the temperature of the sample flow circuits within ±0.10 K. Depending on the applied temperature, the run time of the experiment was varied from 0.05 to 0.2 s. Freshly saturated solutions of CO_2 were prepared by bubbling CO_2 in deionized water. Concentration of CO_2 in the bubbled solution was measured with gas chromatography (GC-6890 from Agilent, Santa Clara, CA, USA) following Shell method®–SMS 2239-04. Fresh water used to dilute the solution in order to maintain the concentration ratio of the amine/amino acid solution 20 times higher than that of the CO_2 solution. This was done to ensure that the reaction conditions with respect to [CO_2] fall within the pseudo first order regime [47]. The

amine/amino acid solutions were also prepared using deionized water. For each run, the CO_2 and amine/amino acid solutions were loaded in two separate syringes. Equal volumes of aqueous solutions of amine/amino acid and CO_2 were mixed in the stopped-flow apparatus. The reaction was monitored by measuring the conductivity change as function of time. The change in the conductivity, Y, with respect to time as described by Knipe et al. [48] was fitted to an exponential equation resembling a first-order kinetics equation:

$$Y = -A.\exp(-k_{ov}.t) + Y_{\infty} \quad (19)$$

where, 'k_{ov}' is the pseudo first-order reaction rate constant. The averages of three experimental runs were considered to obtain a reproducible and consistent k_{ov} value for the whole range of the tested concentrations and temperatures. The reproducibility error of k_{ov} was found to be less than 3% in all experiments. The experimental results were obtained in the provided 'Kinectic Studio' Software (Bradford-on-Avon, Wiltshire, UK). A screenshot of typical conductivity profile is presented in Figure 4.

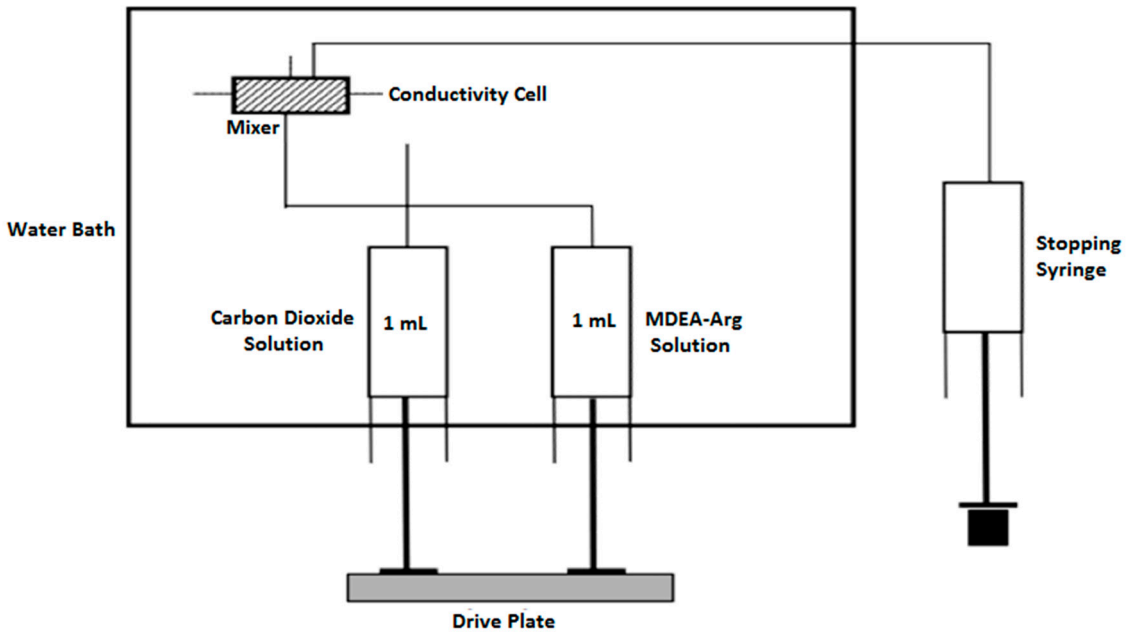

Figure 3. A Schematic Diagram of the Stopped-Flow Apparatus.

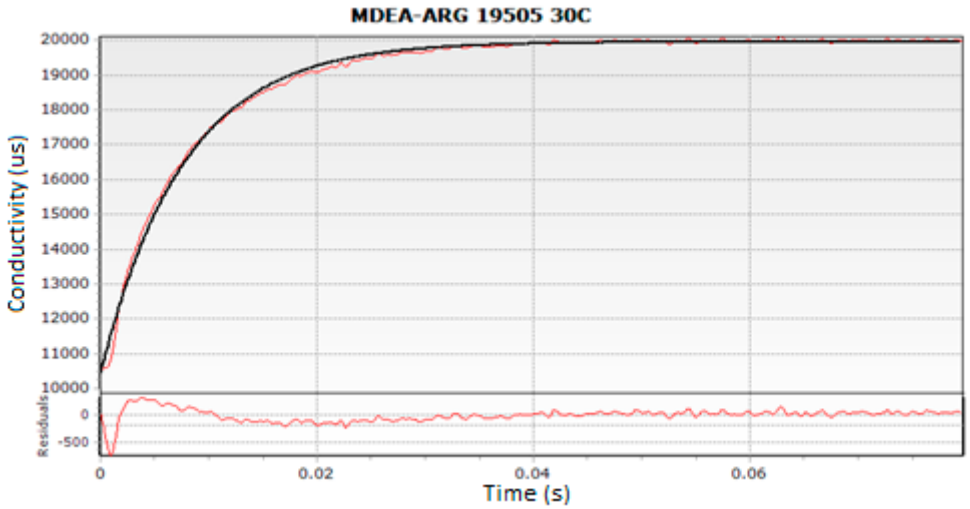

Figure 4. Typical Experimental run for MDEA-Arg at 303 K.

4. Results and Discussion

4.1. Reaction of CO_2 with MDEA and L-Arginine

The obtained pseudo first order rate rate constants, 'k_{ov}', were plotted against temperature for one molar total concentration (see Figure 5). The overall rate constants (k_{ov}) increased with increasing solution temperature as well as with increased [Arg] proportion in the total mixture. Similarly, the plot of the overall rate constants against different Arg/MDEA ratios for a total concentration of 1 mol is shown in Figure 6.

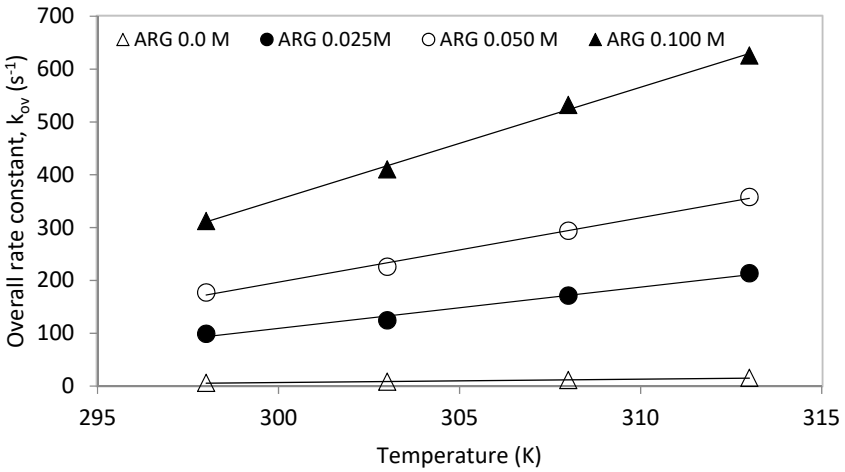

Figure 5. Rate constant, 'k_{ov}', vs. temperature for total 1 M solution.

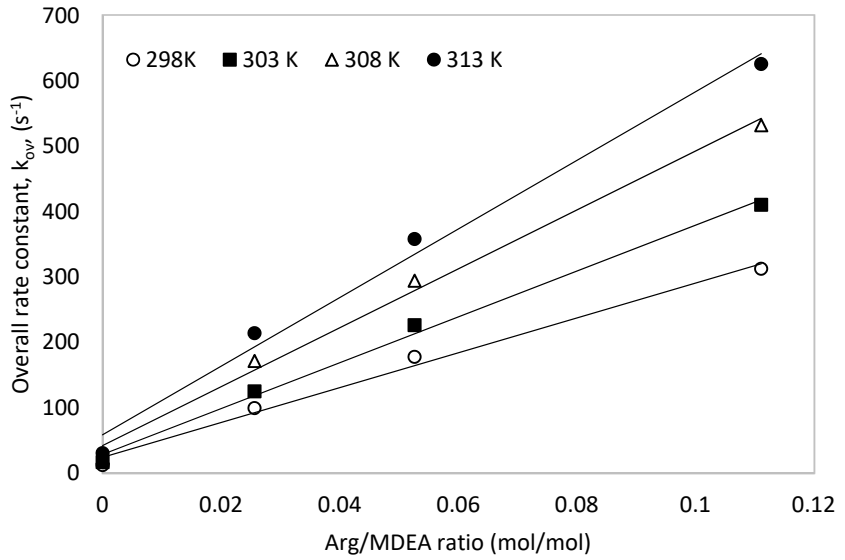

Figure 6. Overall rate constant, 'k_{ov}', vs. different Arg/MDEA ratios for a total 1 M solution.

Upon applying the power law kinetics to plot the overall rate constants against the concentrations of L-Arginine, an average exponent of 0.98 was obtained, which affirms that the pseudo first order regime prevails. Therefore, within the range of the experimental conditions, the reaction can be analysed via the zwitterion mechanism [49]. Additionally, the possibility of using the termolecular mechanism to interpret the obtained data was also verified by plotting k_{ov}/[ARG] against [ARG]. The plots show a satisfactory linear relationship indicating that the termolecular mechanism can also be applied to interpret the obtained experimental kinetics data [49,50]. A typical plot is shown in Figure 7. Hence, obtained experimental kinetics data were analysed using both the zwitterion and termolecular mechanisms.

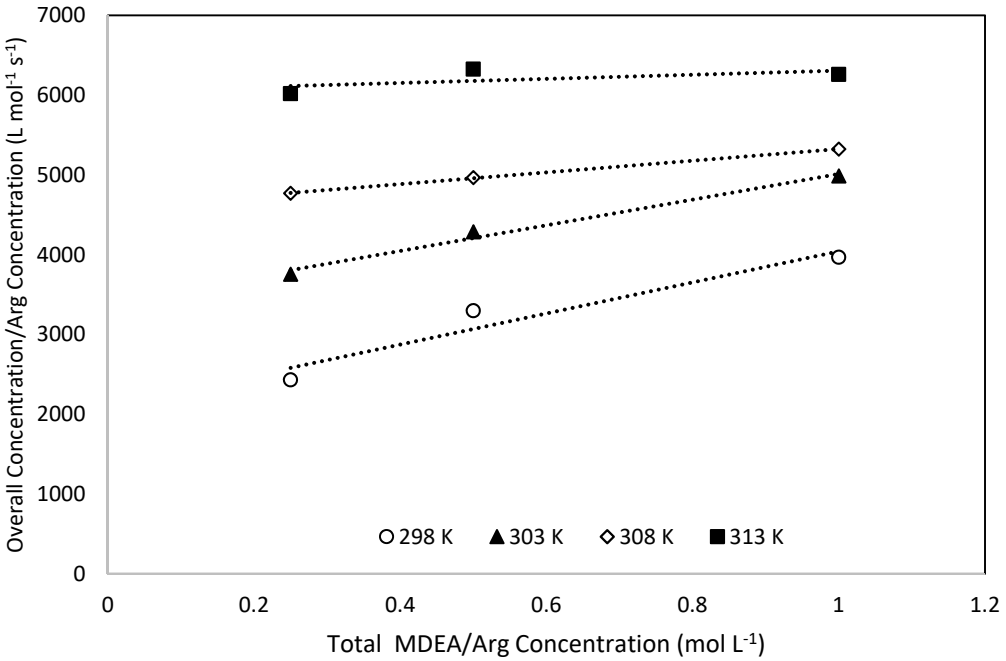

Figure 7. Termolecular mechanism applicability Test for 0.025 M L-Arginine concentration.

4.2. Zwitterion Mechanism

The experimental data of the rate (k_{ov}) of the CO_2 reaction with methyldiethanolamine (MDEA) and L-Arginine (Arg) were obtained by fitting the conductivity-time curves to Equation (19) Zwitterion mechanism was used to interpret the obtained experimental data and the obtained overall rates along with apparent and predicted k_{Arg} rates are presented in Table 1.

Table 1. Rate constants at different temperatures and (MDEA+Arg) concentrations.

ARG	MDEA	$OH \times 10^3$	H_2O	k_{ov}	$k_{Arg\text{-}exp}$	$k_{Arg\text{-}pred}$	AAD%
mol L^{-1}	mol L^{-1}	mol L^{-1}	mol L^{-1}	s^{-1}	s^{-1}	s^{-1}	
			298 K				
0.025	0.975	2.07	49.16	99.17	93.30	80.50	
0.050	0.950	2.07	49.14	177.47	171.70	166.90	
0.100	0.900	2.07	49.08	312.35	306.90	356.00	
0.025	0.475	1.46	52.35	82.40	79.50	70.60	7.60
0.050	0.450	1.46	52.32	152.55	149.80	148.10	
0.100	0.400	1.46	52.26	320.43	318.00	321.80	
0.025	0.225	1.03	53.94	60.75	59.40	65.00	
0.050	0.200	1.03	53.91	125.47	124.30	137.50	
0.075	0.175	1.03	53.88	214.23	213.20	216.90	
			303 K				
0.025	0.975	2.21	49.13	124.65	116.50	104.30	
0.050	0.950	2.21	49.11	226.15	218.20	216.20	
0.100	0.900	2.21	49.05	410.33	402.80	460.40	
0.025	0.475	1.56	52.33	107.15	103.20	91.00	6.30
0.050	0.450	1.56	52.31	195.64	191.90	190.80	
0.100	0.400	1.56	52.25	423.84	420.50	414.30	
0.025	0.225	1.10	53.93	78.32	76.40	83.50	
0.050	0.200	1.10	53.90	165.36	163.70	176.50	
0.075	0.175	1.10	53.88	281.52	280.00	278.40	

Table 1. *Cont.*

ARG	MDEA	OH × 10^3	H_2O	k_{ov}	$k_{Arg\text{-}exp}$	$k_{Arg\text{-}pred}$	AAD%
mol L^{-1}	mol L^{-1}	mol L^{-1}	mol L^{-1}	s^{-1}	s^{-1}	s^{-1}	
			308 K				
0.025	0.975	2.35	49.11	171.38	160.20	136.10	
0.050	0.950	2.35	49.08	294.32	283.40	281.40	
0.100	0.900	2.35	49.03	532.24	521.90	596.90	
0.025	0.475	1.66	52.32	149.90	144.40	117.60	8.20
0.050	0.450	1.66	52.29	234.18	229.00	246.00	
0.100	0.400	1.66	52.24	496.55	491.90	532.50	
0.025	0.225	1.17	53.92	101.41	98.80	106.90	
0.050	0.200	1.17	53.90	231.21	228.90	225.80	
0.075	0.175	1.17	53.87	357.73	355.70	355.80	
			313 K				
0.025	0.975	2.49	49.09	213.71	198.40	167.80	
0.050	0.950	2.49	49.07	357.97	343.10	347.80	
0.100	0.900	2.49	49.02	625.84	611.70	740.80	
0.025	0.475	1.76	52.31	188.23	180.80	145.90	8.40
0.050	0.450	1.76	52.29	310.72	303.70	306.10	
0.100	0.400	1.76	52.24	632.39	626.10	665.10	
0.025	0.225	1.24	53.92	130.31	126.80	133.50	
0.050	0.200	1.24	53.90	302.60	299.50	282.50	
0.075	0.175	1.24	53.87	451.29	448.50	445.90	
			AAD%				7.60

The rate constant k_{arg} was calculated using Equation (17) by subtracting k_{MDEA} and k_{OH} values from k_{ov} values. The values of k_{MDEA}, k_{OH}, k_2, k_a and k_w were estimated from the previous works [41–43,51]. It is to be noted that, there was a typographical error within the power of the previously reported rate expression for k_w ($1.23 \times 10^{12}\ e^{-\frac{4364.7}{T}}$ was reported instead of $1.23 \times 10^{9}\ e^{-\frac{4364.7}{T}}$) [41], this error has been revised in this work and the correct rate expression for k_w along with the other expressions that were used in this work have been listed in Table 2.

Table 2. List of rate expressions used for zwitterion mechanism.

Rate	Equation	References
k_{MDEA} ($m^3\ kmol^{-2}\ s^{-1}$)	$k_2 = 2.56 \times 10^{9} e^{-\frac{5922.0}{T}}$	Benamor et al. [42]
k_{OH} ($m^3\ kmol^{-2}\ s^{-1}$)	$k_{OH} = 4.33 \times 10^{10} e^{-\frac{66666.0}{T}}$	Pinsent et al. [43]
k_2 ($m^3\ kmol^{-1}\ s^{-1}$)	$k_2 = 2.81 \times 10^{10} e^{-\frac{4482.9}{T}}$	Mahmud et al. [41]
k_a ($m^6\ kmol^{-2}\ s^{-1}$)	$k_a = 7.96 \times 10^{10} e^{-\frac{4603.8}{T}}$	Mahmud et al. [41]
k_w ($m^6\ kmol^{-2}\ s^{-1}$)	$k_w = 1.23 \times 10^{9} e^{-\frac{4364.7}{T}}$	Mahmud et al. [41] *

* Corrected value.

Experimental rate constants, 'k_{Arg}', data were fitted to Equation (17) to extract the individual blocks of rate constants described in this equation. The concentrations of water molecules [H_2O] were calculated by mass balance while those of hydroxyl ions [OH^-] were estimated from the relation given by Astarita et al. [52]. The use of this relationship is justified since the CO_2 loading in the amine solution was very small as it was verified by Gas Chromatography throughout all experiments.

$$[OH^-] = \sqrt{\frac{K_W}{K_{Pi}}[AM]} \text{ for } \alpha \leq 10^{-3} \quad (20)$$

Using Equation (20), the total [OH^-] was taken to be the sum of [OH^-] ions produced by MDEA and those produced by Arg. The water dissociation constant, 'K_w' and protonation constant, 'K_{pi}', for MDEA and L-Arginine were expressed as a function of temperature according to the following equation:

$$LnK_i = \frac{a_i}{T} + b_i lnT + c_i T + d_i \quad (21)$$

Values of the constants a_i–d_i are given in Table 3.

Table 3. Values of different equilibrium constant used to estimate OH^- in Equation (20).

Parameter	a_i	b_i	c_i	d_i	Validity Range	Source
$K_{p1(MDEA)}$	−8483.95	−13.8328	0	87.39717	293–333 K	[53]
$K_{p2(Arginine)}$	−3268.3	0	0	−9.9729	293–323 K	[41]
K_w	−13445.9	−22.4773	0	140.932	273–498 K	[54]

Applying a nonlinear regression technique using Excel solver, experimental k_{arg} values were fitted to Equation (17) taking into account the species concentrations, H_2O, Arg, OH^- and MDEA previously calculated. Since the rate expressions for the terms k_2, k_a and k_w were already available from previous work [41]. The regression analysis was initially performed to generate the values of the term k_b and k_{OH} only. However, the obtained values for the k_{OH} indicated no catalytic influence on the k_{Arg} values. This can be attributed to the fact that the concentration of the hydroxyl ions is very low compared to other bases in the system, which leads to the conclusion that there is no significant influence of catalytic hydroxyl ions on the kinetics. Furthermore, the reaction between hydroxyl and CO_2 exhibits slower kinetics which has been previously demonstrated by Gou et al. [55]. Hence, the final regression analysis were performed excluding the k_{OH} term. The generated rate constant values for the k_b term are summarized in Table 4.

Table 4. Reaction rate constants at different temperatures using Zwitterion mechanism.

Temperature	298 K	303 K	308 K	313 K
Rate constant, k_b (m^6 $kmol^{-2}$ s^{-1})	2321.0	3127.5	4400.5	5130

Using these generated rate constants, the overall reaction rate constant, 'k_{Arg}', values were predicted using Equation (17) and were plotted against real experimental data in a parietal plot as shown in Figure 8. It is very clear that the adopted rate model along with extracted individual rate constants represent very well the experimental results with an average absolute deviation, AAD, of 7.6%. Figure 8 validated the choice of the kinetics model used to interpret the data of the reaction of CO_2 with mixtures of MDEA and Arg represented in Equation (12). Furthermore, these results confirm the contribution of Arg and MDEA species in the base-catalytic formation of carbamate.

The individual rate constants at different temperatures were plotted as a function of temperature according to Arrhenius equation as shown in Figure 9 and associated parameters are summarized in Table 5. The activation energy (E_a) of each reaction was derived from the Arrhenius plots along with the pre-exponential coefficient of each rate constant.

From Table 5, it can be observed that the activation energy of L-Arginine (39.15 kJ mol^{-1}) is smaller than that of MDEA (49.24 kJ mol^{-1}), which shows that L-Arginine reacts faster with CO_2 than MDEA. In fact, L-Arginine having a molecular structure similar to that of primary amines, have a faster reaction rate compared to tertiary amine MDEA. The E_a for Arg, MDEA and H_2O catalytic carbamate formation showed that the contribution of water to the overall formation of carbamate (36.29 kJ mol^{-1}) is the most important followed by that of L-Arginine (38.28 kJ mol^{-1}), while the contribution of MDEA to this reaction (42.27 kJ mol^{-1}) were found to be the least.

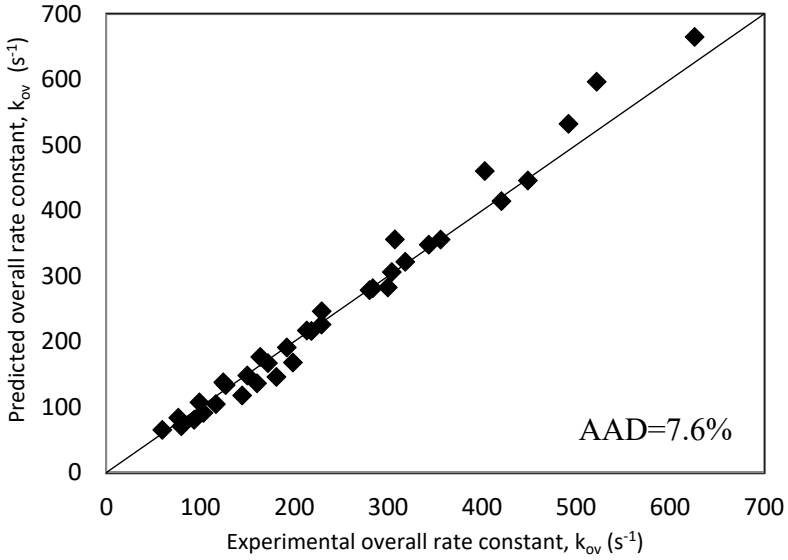

Figure 8. Parity plot of experimental and predicted k_{Arg} values for Zwitterion mechanism.

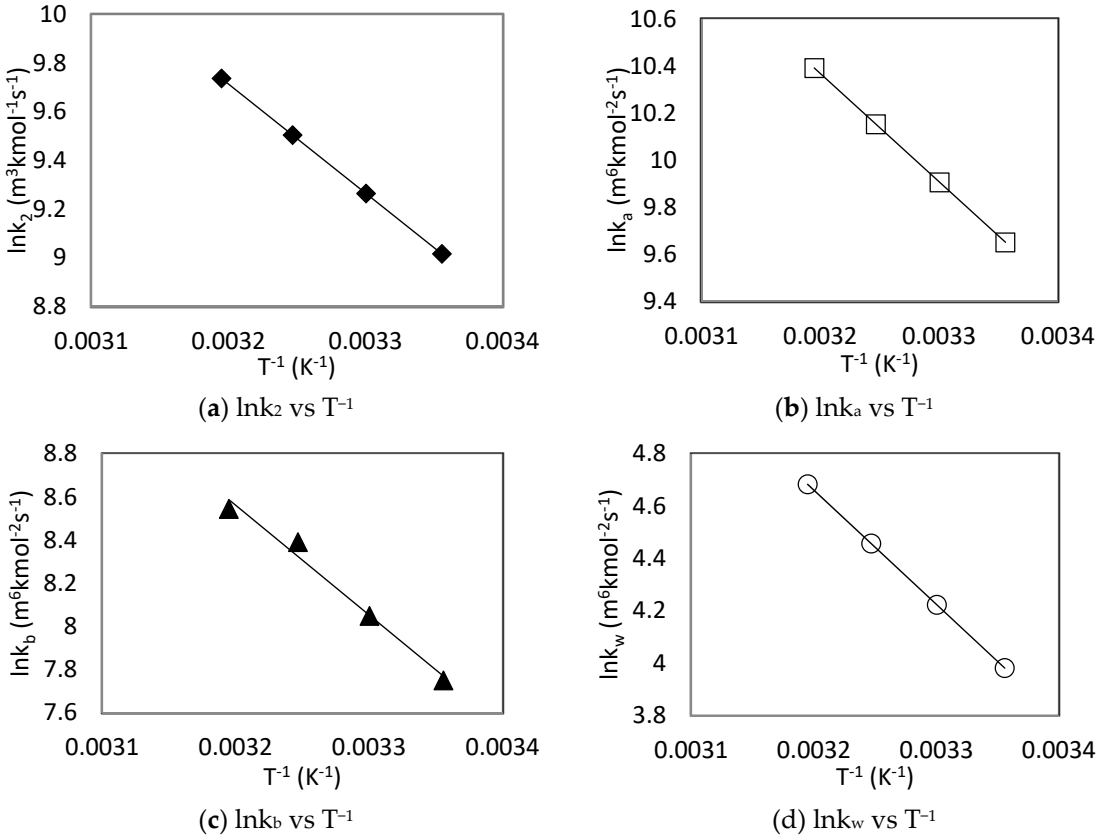

(**a**) $\ln k_2$ vs T^{-1} (**b**) $\ln k_a$ vs T^{-1}

(**c**) $\ln k_b$ vs T^{-1} (d) $\ln k_w$ vs T^{-1}

Figure 9. Arrhenius plots of CO_2-MDEA-Arg rate constants using zwitterion mechanism.

Table 5. Summarized kinetics rate constants for CO_2-MDEA-Arg reaction using Zwitterion Mechanism.

Rate	$k_{ov} = k_{MDEA}[MDEA] + k_{OH^-}[OH^-] + \frac{[Arg]}{\frac{1}{k_2} + \frac{1}{k_a[Arg] + k_b[MDEA] + k_w[H_2O]}}$			References
	Lnk_0	E_a (kJ mol^{-1})	Expression	
k_{MDEA} (m^3 kmol^{-2} s^{-1})	21.66	49.24	$k_{MDEA} = 2.56 \times 10^9 e^{-\frac{5922.0}{T}}$	Benamor et al. [42]
k_{OH} (m^3 kmol^{-2} s^{-1})	24.49	554.26	$k_{OH} = 4.33 \times 10^{10} e^{-\frac{66666.0}{T}}$	Pinsent et al. [43]
k_2 (m^3 kmol^{-2} s^{-1})	24.06	37.27	$k_2 = 2.81 \times 10^{10} e^{-\frac{4482.9}{T}}$	Mahmud et al. [41]
k_a (m^6 kmol^{-2} s^{-1})	25.10	38.28	$k_a = 7.96 \times 10^{10} e^{-\frac{4603.8}{T}}$	Mahmud et al. [41]
k_b (m^6 kmol^{-2} s^{-1})	24.83	42.27	$k_b = 6.07 \times 10^{10} e^{-\frac{5083.8}{T}}$	This Work
k_w (m^6 kmol^{-2} s^{-1})	18.63	36.29	$k_w = 1.23 \times 10^9 e^{-\frac{4364.7}{T}}$	Mahmud et al. [41] *

* Corrected expression.

4.3. Termolecular Mechanism

Since the termolecular applicability tests revealed the possibility of applying this mechanism to interpret the experimental data, the kinetics of CO_2-MDEA-Arg were then further investigated via this mechanism. Similar to that of the zwitterion mechanism, the values of k_a and k_w were also estimated from previous work [41] and are listed in Table 6.

Table 6. List of rate expressions used for Termolecular mechanism.

Rate	Equation	References
k_a (m^6 kmol^{-2} s^{-1})	$k_a = 5.72 \times 10^{10} e^{-\frac{4769.00}{T}}$	Mahmud et al. [4]
k_w (m^6 kmol^{-2} s^{-1})	$k_w = 9.41 \times 10^7 e^{-\frac{4365.00}{T}}$	Mahmud et al. [41]

Using the k_a and k_w values, previously obtained k_{Arg} values were then fitted in accordance to the Equation (18). Excel solver was then used to regress the experimental data to obtain the rate expressions. The apparent and predicted k_{Arg} values obtained using the termolecular mechanism are presented in Table 7.

Similar to the results obtained using the zwitterion mechanism, the obtained fitting results showed that hydroxyl ion (k_{hyd}) had a negligible effect for CO_2-MDEA-Arginine reaction using termolecular mechanism. Only L-Arginine, MDEA and water concentrations effects were found to be significant. The natural logarithm of the individual rate constants was plotted against T^{-1} according to Arrhenius equation as shown in Figure 10. The generated rate constant values for the k_b term are summarized in Table 8.

The predicted rate constant values were compared to the experimental ones as via a parity plot shown in Figure 11, which displayed good agreement between both values with an AAD of 8.0%. Since the AAD% is very close to that obtained in case of zwitterion mechanism (7.60%), it can be suggested that termolecular mechanism can be also used to interpret the obtained experimental data. The obtained rate expressions using termolecular are summarized in Table 9.

Table 7. Rate constants at different temperatures and (MDEA+Arg) concentrations.

ARG	MDEA	OH	H_2O	$k_{Arg\text{-}exp}$	$k_{Arg\text{-}pred}$	AAD%
mol L^{-1}	mol L^{-1}	mol L^{-1}	mol L^{-1}	s^{-1}	s^{-1}	
			298 K			
0.025	0.975	3.2×10^{-4}	49.16	93.3	79.7	
0.050	0.950	4.5×10^{-4}	49.14	171.8	166.2	
0.100	0.900	6.2×10^{-4}	49.08	306.9	358.9	
0.025	0.475	2.3×10^{-4}	52.35	79.5	70.0	7.8
0.050	0.450	3.1×10^{-4}	52.32	149.8	146.6	
0.100	0.400	4.1×10^{-4}	52.26	318.0	319.9	
0.025	0.225	1.5×10^{-4}	53.94	59.4	65.1	
0.050	0.200	2.1×10^{-4}	53.91	124.3	136.8	
0.075	0.175	2.4×10^{-4}	53.88	213.2	215.2	
			303 K			
0.025	0.975	3.0×10^{-4}	49.16	116.5	103.4	
0.050	0.950	4.2×10^{-4}	49.14	218.2	215.3	
0.100	0.900	5.8×10^{-4}	49.08	402.8	465.2	
0.025	0.475	2.1×10^{-4}	52.35	103.2	90.0	6.9
0.050	0.450	2.9×10^{-4}	52.32	191.9	188.7	
0.100	0.400	3.8×10^{-4}	52.26	420.5	411.9	
0.025	0.225	1.4×10^{-4}	53.94	76.4	83.4	
0.050	0.200	1.9×10^{-4}	53.91	163.7	175.4	
0.075	0.175	2.2×10^{-4}	53.88	280.1	276.0	
			308 K			
0.025	0.98	2.8×10^{-4}	49.16	160.2	134.7	
0.050	0.95	3.9×10^{-4}	49.14	283.4	280.3	
0.100	0.90	5.4×10^{-4}	49.08	521.9	604.6	
0.025	0.48	2.0×10^{-4}	52.35	144.5	115.8	8.6
0.050	0.45	2.7×10^{-4}	52.32	229.0	242.6	
0.100	0.40	3.6×10^{-4}	52.26	492.0	529.2	
0.025	0.23	1.3×10^{-4}	53.94	98.8	106.4	
0.050	0.20	1.8×10^{-4}	53.91	228.9	223.8	
0.075	0.18	2.1×10^{-4}	53.88	355.7	352.2	
			313 K			
0.025	0.98	2.6×10^{-4}	49.16	198.5	164.8	
0.050	0.95	3.6×10^{-4}	49.14	343.1	343.9	
0.100	0.90	5.0×10^{-4}	49.08	611.8	745.2	
0.025	0.48	1.8×10^{-4}	52.35	180.8	143.3	8.8
0.050	0.45	2.5×10^{-4}	52.32	303.7	301.0	
0.100	0.40	3.3×10^{-4}	52.26	626.1	659.5	
0.025	0.23	1.3×10^{-4}	53.94	126.8	132.6	
0.050	0.20	1.7×10^{-4}	53.91	299.5	279.6	
0.075	0.18	1.9×10^{-4}	53.88	448.6	441.0	
			Overall AAD%			8.0

Table 8. Reaction rate constants at different temperatures using termolecular mechanism.

Rate Constant	298 K	303 K	308 K	313 K
k_b (m^6 $kmol^{-2}$ s^{-1})	1043.0	1397.0	1927.0	2240.0

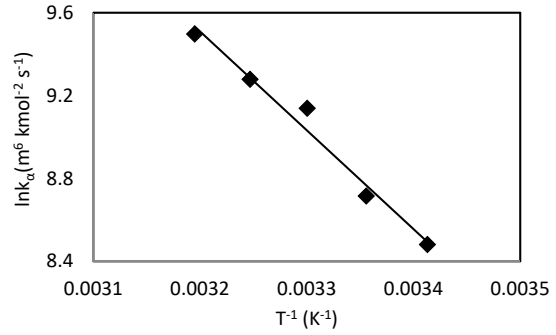

(**a**) lnk$_a$ vs T^{-1}

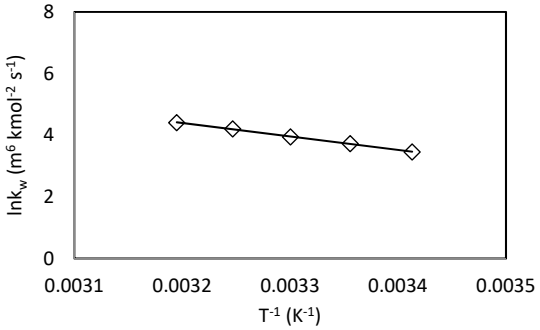

(**b**) lnk$_w$ vs T^{-1}

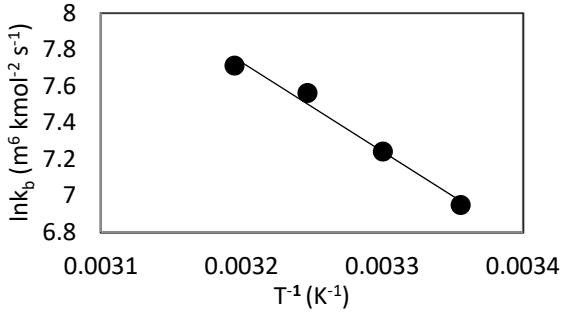

(**c**) lnk$_b$ vs T^{-1}

Figure 10. Arrhenius plots of CO_2-MDEA-Arg rate constants using termolecular mechanism.

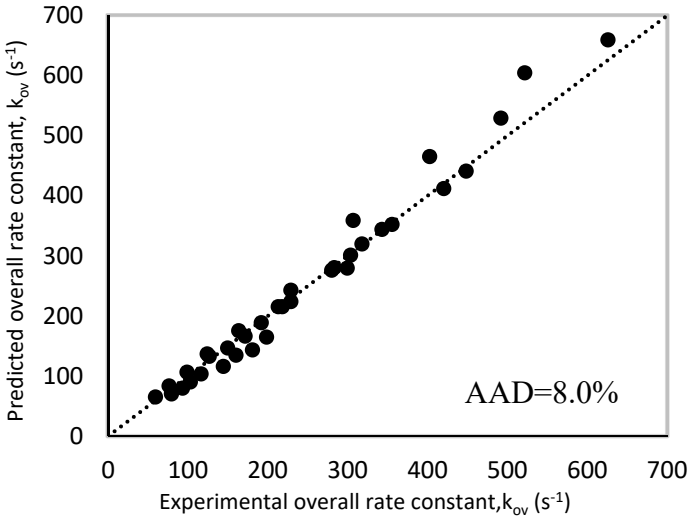

Figure 11. Parity plot of experimental and predicted 'k_{Arg}' values for termolecular mechanism.

Table 9. Summarized kinetics rate constants for CO_2-MDEA-Arg reaction using Termolecular Mechanism.

Rate	$k_{ov} = k_{MDEA}[MDEA] + k_{OH^-}[OH^-] + k_a[Arg] + k_b[MDEA] + k_w[H_2O]$			References
	$\ln k_0$	E_a (kJ mol^{-1})	Expression	
k_{MDEA} (m^3 kmol^{-2} s^{-1})	21.66	49.24	$k_{MDEA} = 2.56 \times 10^9 e^{-\frac{5922.0}{T}}$	Benamor et al. [42]
k_{OH} (m^3 kmol^{-2} s^{-1})	24.49	554.26	$k_{OH} = 4.33 \times 10^{10} e^{-\frac{66666.0}{T}}$	Pinsent et al. [43]
k_a (m^6 kmol^{-2} s^{-1})	24.77	38.28	$k_a = 5.72x \times 10^{10} e^{-\frac{4769.0}{T}}$	Mahmud et al. [41]
k_b (m^6 kmol^{-2} s^{-1})	23.38	40.65	$k_b = 1.42 \times 10^{10} e^{-\frac{4888.6}{T}}$	This Work
k_w (m^6 kmol^{-2} s^{-1})	18.63	36.29	$k_w = 9.41 \times 10^7 e^{-\frac{4365.0}{T}}$	Mahmud et al. [41]

Upon evaluating the obtained rate expression for the 'k_b' term in both mechanisms, it is observed that activation energies in both models are comparable to each other ($E_a{}^Z$ = 42.27 kJ mol^{-1} and $E_a{}^T$ = 40.65 kJ mol^{-1}). Furthermore, it is noticed that regardless of the model used catalytic effect of L-Arginine ($E_a{}^Z$ = $E_a{}^T$ = 38.28 kJ mol^{-1}) is higher than the catalytic effect of MDEA. Based on this, it can be concluded that the CO_2-MDEA-Arg reactions can be effectively interpreted using both zwitterion and termolecular mechanisms.

5. Comparison with Other Amine Systems

5.1. Comparison with Secondary, Tertiary and Sterically Hindered Amine

The obtained rate constants data for 1M MDEA-Arg (0.9M MDEA + 0.1M Arg) in this work were compared with those of DEA [56], MDEA [42] and AMP [57] as shown in Figure 12. It was observed that the rate constants of MDEA-Arg were much lower than that of secondary amine (DEA) and lower than that of sterically hindered amine (AMP). However, the rate constant of MDEA-Arg mixtures were always higher than those of the tertiary amine (MDEA). This elucidates the effect of L-Arginine presence in the MDEA-Arg blend which can enhance the overall kinetics of the CO_2-MDEA reaction and make it comparable to other secondary and hindered amines. Based on the above analysis, the overall rate constants of these amine systems with CO_2 were found to be in the following order: DEA > AMP > MDEA-Arg > MDEA.

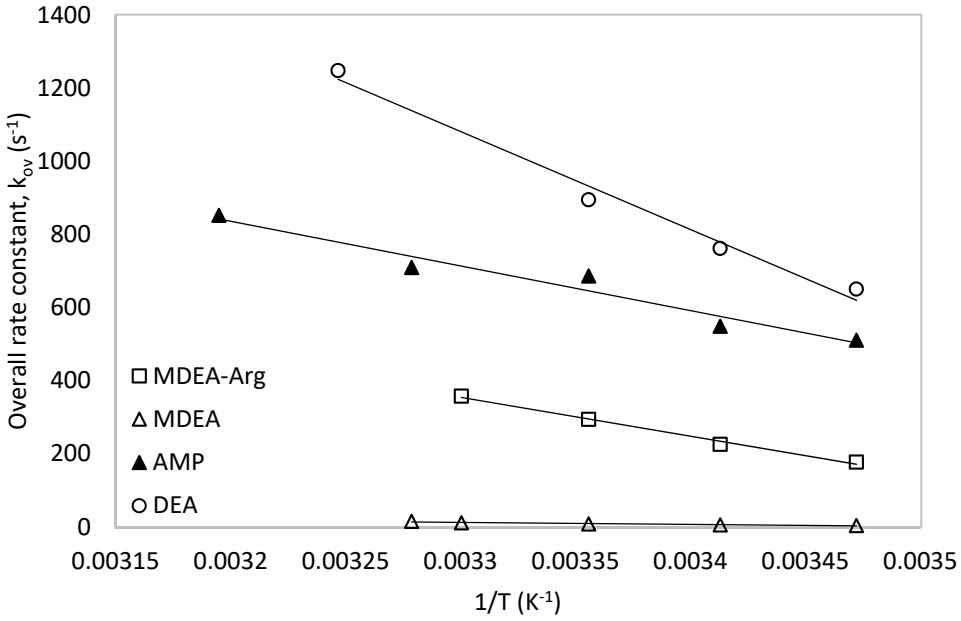

Figure 12. Comparison of the obtained data with MDEA-Arg with other amine systems.

5.2. Comparison of the Promoting Effect of L-Arginine

The promoting effect of L-Arginine investigated in this work was also compared with that of the available data of MDEA-Glycine [42] and MDEA-DEA [58] systems at different temperatures and at the same overall concentration (1 M) as shown in Figure 13. For all three compared systems, the same 0.1 M of the promoter was added. It is observed that the addition of 0.1 M L-Arginine in the MDEA-Arg has resulted in higher overall rate constant compared to the addition of the 0.1 M DEA. However, the addition of 0.1 M Glycine in the MDEA blend has resulted in higher overall rate constant compared to that of 0.1 M L-Arginine. Although the previous study [41] revealed that the kinetics of L-Arginine alone with CO_2 is higher than that of the Glycine, Guo et al. [55] observed that the Glycine at higher pH exhibits faster kinetics. Since the presence of MDEA can increase pH of the solution, it triggers the base form of Glycine to react with the CO_2 resulting in a higher overall rate constant in the MDEA-Glycine blend as observed in the work of Benamor et al. [42]. The presence of MDEA has more significant catalytic effect towards the formation of zwitterion intermediate in MDEA-Glycine (E_a = 24.67 kJ mol^{-1} [42]) compared to that of MDEA-Arg (E_a = 42.27 kJ mol^{-1}). Furthermore, activation energy for the reaction of zwitterion intermediate formation of Glycine in the MDEA-Gly is 22.95 kJ mol^{-1} [42] is also lower than that of L-Arginine (E_a = 37.27 kJ mol^{-1}) in the MDEA-Arg blend. Therefore, based on this analysis, the rate constants of the three blended amine systems with CO_2 were found to be in the following order: MDEA-Gly > MDEA-Arg > MDEA-DEA.

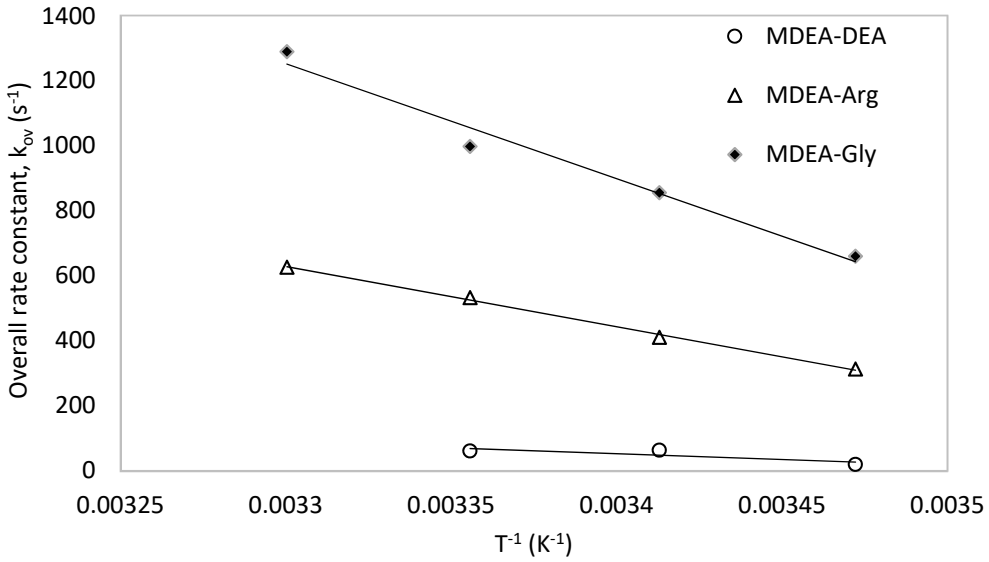

Figure 13. Comparison of MDEA-Arg with other MDEA blends.

6. Conclusions

The kinetics of the reaction of CO_2 with MDEA + Arginine in aqueous solutions was studied using the stopped-flow technique for the first time. The measurements were performed for a concentration range from 0.25 M to 1 M and a temperature range from 298 to 313 K. The rate constants were well correlated by Arrhenius equation type. The activation energies for the rate constants were estimated. Both of the adopted zwitterion and termolecular models were very accurate in representing the experimental data over a range of five different temperatures from 293 to 313 K with an AAD of 7.6% and 8.0%, respectively. The contribution of L-Arginine, MDEA and H_2O to the catalytic carbamate formation pathway was assessed using rate constants generated form the reaction of arginine alone with CO_2. The results showed that the contribution of arginine to the overall formation is more significant followed by the contribution of water in both models, while the contribution of MDEA molecules was found to be the least. Based on the regression results, rate expression for the catalytic formation of zwitterion was to be $k_b = 6.07 \times 10^{10} e^{-\frac{5083.8}{T}}$ for the zwitterion

mechanism and $k_b = 1.42 \times 10^{10} e^{-\frac{4888.6}{T}}$ for the termolecular mechanism. A comparison of the obtained overall rate constant with other amine systems revealed the MDEA-Arginine-CO_2 reaction was faster than that of MDEA-CO_2 but slower than that of secondary and sterically hindered amine. A further comparison with MDEA-promotor blends showed that the reaction of MDEA-Arginine with CO_2 is slower than MDEA-Glycine but faster than MDEA-DEA. This was attributed to the fact that the catalytic contribution of L-Arginine for the formation of zwitterion intermediate is lower compared to Glycine in MDEA blends. Furthermore, presence of MDEA can significantly catalyse the formation zwitterion intermediate in MDEA-Glycine blend (E_a = 24.67 kJ mol^{-1} [43]) than that of MDEA-Arg blend (E_a = 42.27 kJ mol^{-1}). Consequently, a faster reaction kinetics was observed in MDEA-Glycine-CO_2 reactions than MDEA-Arg-CO_2 reactions.

Author Contributions: Conceptualization, A.B., N.M., and P.T.; Methodology, A.B. and N.M.; Software, A.B.; Validation, A.B., N.M., M.N., M.H.E.-N. and P.T.; Formal Analysis, A.B., N.M, M.N. and M.H.E.-N.; Investigation, A.B., N.M. and M.H.E.-N.; Resources, A.B.; Data Curation, A.B., N.M. and M.N.; Writing-Original Draft Preparation, N.M., and A.B.; Writing-Review & Editing, N.M., A.B., M.N., M.H.E.-N. and P.T.; Visualization, A.B., M.N. and N.M.; Supervision, A.B. and P.T.; Project Administration, A.B. and M.H.E.-N.; Funding Acquisition, A.B.

Funding: This paper was made possible by an NPRP Grant # 7 - 1154 - 2 – 433 from the Qatar National Research Fund (a member of Qatar Foundation). The statements made herein are solely the responsibility of the authors.

Acknowledgments: The authors thank Ahmed Soliman and Dan Jerry Cortes for providing laboratory support.

Conflicts of Interest: The authors declare no conflict of interest.

Nomenclature

MDEA	N-methyldiethanolamine
Arg	L-Arginine
Gly	Glycine
MEA	Monoethanolamine
DEA	Diethanolamine
AMP	2-Amino-2-Methyl-1-Propanol
$r_{CO_2\text{-MDEA}}$ (l mol^{-1} s^{-1})	Reaction rate of CO_2 with MDEA
$r_{CO_2\text{-OH}}$ (l mol^{-1} s^{-1})	Reaction rate of CO_2 with hydroxyl ions
$r_{CO_2\text{-OH}}$ (l mol^{-1} s^{-1})	Reaction rate of CO_2 with L-Arginine
r_{CO_2} (l mol^{-1} s^{-1})	Reaction rate of CO_2 with MDEA-Arginine
k_{MDEA} (s^{-1})	Overall reaction rate of CO_2 and MDEA
k_{OH} (s^{-1})	Overall reaction rate of CO_2 and Hydroxyl ion
k_{Arg} (s^{-1})	Overall reaction rate of CO_2 and L-Arginine
k_{ov} (s^{-1})	Overall reaction rate with CO_2 with MDEA and L-Arginine
k_1 (m^3 $kmol^{-1}$ s^{-1})	Reaction rate constant of the formation of the intermediate Zwitterion
K_{MDEA} (m^3 $kmol^{-1}$ s^{-1})	Reaction rate constant of CO_2 and MDEA reaction.
K_{OH} (m^3 $kmol^{-1}$ s^{-1})	Reaction rate constant of CO_2 and hydroxyl ion reaction.
k_{-1} (s^{-1})	Reaction rate constant of the consumption of the intermediate Zwitterion
$k_{b,I}$ (s^{-1})	Individual reaction rate constants according to zwitterion mechanism
T (K)	Temperature
t (s)	Time
K_w (mol l^{-1})	Water dissociation constant
K_{Pi} (mol l^{-1})	Protonation constant for MDEA and L-Arginine
$k_{Arg\text{-}exp}$ (s^{-1})	Experimental apparent rate constant of CO_2 and L-Arginine.
$k_{Arg\text{-}pred}$ (s^{-1})	Predicted apparent rate constant of CO_2 and L-Arginine.
E_a (kJ mol^{-1})	Activation energy
$E_a{}^Z$ (kJ mol^{-1})	Activation energy obtained in zwitterion mechanism
$E_a{}^T$ (kJ mol^{-1})	Activation energy obtained in termolecular mechanism
k_a (m^6 $kmol^{-2}$ s^{-1})	Catalytic contribution of L-Arginine in the reaction rate according to zwitterion mechanism
k_{hyd} (m^6 $kmol^{-2}$ s^{-1})	Catalytic contribution of hydroxyl ion in the reaction rate according to zwitterion mechanism
k_b (m^6 $kmol^{-2}$ s^{-1})	Catalytic contribution of MDEA in the reaction rate according to zwitterion mechanism

References

1. Tontiwachwuthikul, P.; Idem, R.; Gelowitz, D.; Liang, Z.H.; Supap, T.; Chan, C.W.; Sanpasertparnich, T.; Saiwan, C.; Smithson, H. Recent progress and new development of post-combustion carbon-capture technology using reactive solvents. *Carbon Manag.* **2011**, *2*, 261–263. [CrossRef]
2. Zhou, Q.; Chan, C.W.; Tontiwachiwuthikul, P.; Idem, R.; Gelowitz, D. A statistical analysis of the carbon dioxide capture process. *Int. J. Greenh. Gas Control* **2009**, *3*, 535–544. [CrossRef]
3. Rubin, E.S.; Mantripragada, H.; Marks, A.; Versteeg, P.; Kitchin, J. The outlook for improved carbon capture technology. *Prog. Energy Combust. Sci.* **2012**, *38*, 630–671. [CrossRef]
4. Lee, A.S.; Kitchin, J.R. Chemical and Molecular Descriptors for the Reactivity of Amines with CO_2. *Ind. Eng. Chem. Res.* **2012**, *51*, 13609–13618. [CrossRef]
5. Zhang, Z.; Borhani, T.N.G.; El-Naas, M.H. Chapter 4.5—Carbon Capture. In *Exergetic, Energetic and Environmental Dimensions*; Dincer, I., Colpan, C.O., Kizilkan, O., Eds.; Academic Press: Cambridge, MA, USA, 2018; pp. 997–1016. ISBN 978-0-12-813734-5.
6. Zhang, Z.; Yan, Y.; Chen, Y.; Zhang, L. Investigation of CO_2 absorption in methyldiethanolamine and 2-(1-piperazinyl)-ethylamine using hollow fiber membrane contactors: Part, C. Effect of operating variables. *J. Nat. Gas Sci. Eng.* **2014**, *20*, 58–66. [CrossRef]
7. Chakravarty, T.; Phukan, U.K.; Weiland, R.H. Reaction of Acid Gases with mixtures of amines. *Chem. Eng. Prog.* **1985**, *81*, 32–36.
8. Liang, Z.; Rongwong, W.; Liu, H.; Fu, K.; Gao, H.; Cao, F.; Zhang, R.; Sema, T.; Henni, A.; Sumon, K.; et al. Recent progress and new developments in post-combustion carbon-capture technology with amine based solvents. *Int. J. Greenh. Gas Control* **2015**, *40*, 26–54. [CrossRef]
9. Benamor, A.; Ali, B.S.; Aroua, M.K. Kinetic of CO_2 absorption and carbamate formation in aqueous solutions of diethanolamine. *Korean J. Chem. Eng.* **2008**, *25*, 451–460. [CrossRef]
10. Zhao, X.; Cui, Q.; Wang, B.; Yan, X.; Singh, S.; Zhang, F.; Gao, X.; Li, Y. Recent progress of amine modified sorbents for capturing CO_2 from flue gas. *Chin. J. Chem. Eng.* **2018**, *26*, 2292–2302. [CrossRef]
11. Wang, Q.; Luo, J.; Zhong, Z.; Borgna, A. CO_2 capture by solid adsorbents and their applications: Current status and new trends. *Energy Environ. Sci.* **2011**, *4*, 42–55. [CrossRef]
12. Munoz, D.M.; Portugal, A.F.; Lozano, A.E.; de la Campa, J.G.; de Abajo, J. New liquid absorbents for the removal of CO_2 from gas mixtures. *Energy Environ. Sci.* **2009**, *2*, 883–891. [CrossRef]
13. Brœder, P.; Svendsen, H.F. Capacity and Kinetics of Solvents for Post-Combustion CO_2 Capture. *Energy Procedia* **2012**, *23*, 45–54. [CrossRef]
14. Puxty, G.; Rowland, R.; Allport, A.; Yang, Q.; Bown, M.; Burns, R.; Maeder, M.; Attalla, M. Carbon Dioxide Postcombustion Capture: A Novel Screening Study of the Carbon Dioxide Absorption Performance of 76 Amines. *Environ. Sci. Technol.* **2009**, *43*, 6427–6433. [CrossRef]
15. Zhang, Z.; Li, Y.; Zhang, W.; Wang, J.; Soltanian, M.R.; Olabi, A.G. Effectiveness of amino acid salt solutions in capturing CO_2: A review. *Renew. Sustain. Energy Rev.* **2018**, *98*, 179–188. [CrossRef]
16. Lerche, B.M. *CO_2 Capture from Flue Gas Using Amino Acid Salt Solutions*; Department of Chemical and Biochemical Engineering, Technical University of Denmark: Kongens Lyngby, Denmark, 2012.
17. Goetheer, E.; Nell, L. First pilot results from TNO's solvent development workflow. *Carbon Capture J.* **2009**, *8*, 2–3.
18. Eide-Haugmo, I.; Brakstad, O.G.; Hoff, K.A.; da Silva, E.F.; Svendsen, H.F. Marine biodegradability and ecotoxicity of solvents for CO 2-capture of natural gas. *Int. J. Greenh. Gas Control* **2012**, *9*, 184–192. [CrossRef]
19. Aronu, U.E.; Svendsen, H.F.; Hoff, K.A. Investigation of amine amino acid salts for carbon dioxide absorption. *Int. J. Greenh. Gas Control* **2010**, *4*, 771–775. [CrossRef]
20. Kumar, P.; Hogendoorn, J.; Versteeg, G.; Feron, P. Kinetics of the reaction of CO_2 with aqueous potassium salt of taurine and glycine. *AIChE J.* **2003**, *49*, 203–213. [CrossRef]
21. Kumar, P.; Hogendoorn, J.; Feron, P.; Versteeg, G. Equilibrium solubility of CO_2 in aqueous potassium taurate solutions: Part 1. Crystallization in carbon dioxide loaded aqueous salt solutions of amino acids. *Ind. Eng. Chem. Res.* **2003**, *42*, 2832–2840. [CrossRef]
22. Aronu, U.E.; Hessen, E.T.; Haug-Warberg, T.; Hoff, K.A.; Svendsen, H.F. Vapor–liquid equilibrium in amino acid salt system: Experiments and modeling. *Chem. Eng. Sci.* **2011**, *66*, 2191–2198. [CrossRef]

23. Kumar, P.; Hogendoorn, J.; Timmer, S.; Feron, P.; Versteeg, G. Equilibrium solubility of CO_2 in aqueous potassium taurate solutions: Part 2. Experimental VLE data and model. *Ind. Eng. Chem. Res.* **2003**, *42*, 2841–2852. [CrossRef]
24. Majchrowicz, M.; Brilman, D. Solubility of CO_2 in aqueous potassium l-prolinate solutions—Absorber conditions. *Chem. Eng. Sci.* **2012**, *72*, 35–44. [CrossRef]
25. Portugal, A.F.; Sousa, J.M.; Magalhães, F.D.; Mendes, A. Solubility of carbon dioxide in aqueous solutions of amino acid salts. *Chem. Eng. Sci.* **2009**, *64*, 1993–2002. [CrossRef]
26. Schneider, R.; Schramm, H. Environmentally friendly and economic carbon capture from power plant flue gases. In Proceedings of the 1st Post Combustion Capture Conference, Abu Dhabi, UAE, 17–19 May 2011.
27. Park, S.-W.; Son, Y.-S.; Park, D.-W.; Oh, K.-J. Absorption of carbon dioxide into aqueous solution of sodium glycinate. *Sep. Sci. Technol.* **2008**, *43*, 3003–3019. [CrossRef]
28. Lee, S.; Song, H.-J.; Maken, S.; Park, J.-W. Kinetics of CO_2 absorption in aqueous sodium glycinate solutions. *Ind. Eng. Chem. Res.* **2007**, *46*, 1578–1583. [CrossRef]
29. Shen, S.; Yang, Y.-N.; Bian, Y.; Zhao, Y. Kinetics of CO_2 Absorption into Aqueous Basic Amino Acid Salt: Potassium Salt of Lysine Solution. *Environ. Sci. Technol.* **2016**, *50*, 2054–2063. [CrossRef]
30. Shen, S.; Yang, Y.-n.; Zhao, Y.; Bian, Y. Reaction kinetics of carbon dioxide absorption into aqueous potassium salt of histidine. *Chem. Eng. Sci.* **2016**, *146*, 76–87. [CrossRef]
31. Portugal, A.; Derks, P.; Versteeg, G.; Magalhaes, F.; Mendes, A. Characterization of potassium glycinate for carbon dioxide absorption purposes. *Chem. Eng. Sci.* **2007**, *62*, 6534–6547. [CrossRef]
32. Portugal, A.; Magalhaes, F.; Mendes, A. Carbon dioxide absorption kinetics in potassium threonate. *Chem. Eng. Sci.* **2008**, *63*, 3493–3503. [CrossRef]
33. Hwang, K.-S.; Park, D.-W.; Oh, K.-J.; Kim, S.-S.; Park, S.-W. Chemical Absorption of Carbon Dioxide into Aqueous Solution of Potassium Threonate. *Sep. Sci. Technol.* **2010**, *45*, 497–507. [CrossRef]
34. Wei, C.-C.; Puxty, G.; Feron, P. Amino acid salts for CO_2 capture at flue gas temperatures. *Chem. Eng. Sci.* **2014**, *107*, 218–226. [CrossRef]
35. Aronu, U.E.; Hartono, A.; Svendsen, H.F. Density, viscosity and N2O solubility of aqueous amino acid salt and amine amino acid salt solutions. *J. Chem. Thermodyn.* **2012**, *45*, 90–99. [CrossRef]
36. Kumar, P.S.; Hogendoorn, J.; Feron, P.; Versteeg, G. Density, viscosity, solubility and diffusivity of N2O in aqueous amino acid salt solutions. *J. Chem. Eng. Data* **2001**, *46*, 1357–1361. [CrossRef]
37. Hamborg, E.S.; Niederer, J.P.; Versteeg, G.F. Dissociation constants and thermodynamic properties of amino acids used in CO_2 absorption from (293 to 353) K. *J. Chem. Eng. Data* **2007**, *52*, 2491–2502. [CrossRef]
38. Hamborg, E.S.; van Swaaij, W.P.; Versteeg, G.F. Diffusivities in aqueous solutions of the potassium salt of amino acids. *J. Chem. Eng. Data* **2008**, *53*, 1141–1145. [CrossRef]
39. Van Holst, J.; Versteeg, G.; Brilman, D.; Hogendoorn, J. Kinetic study of CO_2 with various amino acid salts in aqueous solution. *Chem. Eng. Sci.* **2009**, *64*, 59–68. [CrossRef]
40. Dalton, J.B.; Schmidt, C.L. The solubilities of certain amino acids in water, the densities of their solutions at twenty-five degrees and the calculated heats of solution and partial molal volumes. *J. Biol. Chem.* **1933**, *103*, 549–578.
41. Mahmud, N.; Benamor, A.; Nasser, M.S.; Al-Marri, M.J.; Qiblawey, H.; Tontiwachwuthikul, P. Reaction kinetics of carbon dioxide with aqueous solutions of l-Arginine, Glycine & Sarcosine using the stopped flow technique. *Int. J. Greenh. Gas Control* **2017**, *63*, 47–58. [CrossRef]
42. Benamor, A.; Al-Marri, M.J.; Khraisheh, M.; Nasser, M.S.; Tontiwachwuthikul, P. Reaction kinetics of carbon dioxide in aqueous blends of N-methyldiethanolamine and glycine using the stopped flow technique. *J. Nat. Gas Sci. Eng.* **2016**, *33*, 186–195. [CrossRef]
43. Pinsent, B.R.W.; Pearson, L.; Roughton, F.J.W. The kinetics of combination of carbon dioxide with hydroxide ions. *Trans. Faraday Soc.* **1956**, *52*, 1512–1520. [CrossRef]
44. Caplow, M. Kinetics of carbamate formation and breakdown. *J. Am. Chem. Soc.* **1968**, *90*, 6795–6803. [CrossRef]
45. Crooks, J.E.; Donnellan, J.P. Kinetics and mechanism of the reaction between carbon dioxide and amines in aqueous solution. *J. Chem. Soc. Perkin Trans.* **1989**, *2*, 331–333. [CrossRef]
46. Da Silva, E.F.; Svendsen, H.F. Computational chemistry study of reactions, equilibrium and kinetics of chemical CO_2 absorption. *Int. J. Greenh. Gas Control* **2007**, *1*, 151–157. [CrossRef]
47. Ali, S.H.; Merchant, S.Q.; Fahim, M.A. Kinetic study of reactive absorption of some primary amines with carbon dioxide in ethanol solution. *Sep. Purifi. Technol.* **2000**, *18*, 163–175. [CrossRef]

48. Knipe, A.C.; McLean, D.; Tranter, R.L. A fast response conductivity amplifier for chemical kinetics. *J. Phys. E Sci. Instrum.* **1974**, *7*, 586–590. [CrossRef]
49. Alper, E.; Bouhamra, W. Kinetics and mechanisms of reaction between carbon disulphide and morpholine in aqueous solutions. *Chem. Eng. Technol.* **1994**, *17*, 138–140. [CrossRef]
50. Vaidya, P.D.; Kenig, E.Y. Termolecular Kinetic Model for CO_2-Alkanolamine Reactions: An Overview. *Chem. Eng. Technol.* **2010**, *33*, 1577–1581. [CrossRef]
51. Peters, L.; Hussain, A.; Follmann, M.; Melin, T.; Hägg, M.B. CO_2 removal from natural gas by employing amine absorption and membrane technology—A technical and economical analysis. *Chem. Eng. J.* **2011**, *172*, 952–960. [CrossRef]
52. Astaria, G.; Savage, D.W.; Bisio, A. *Gas Treating with Chemical Solvents*; John Wiley & Sons Inc.: New York, NY, USA, 1983; ISBN 978-0471057680.
53. Littel, R.J.; Bos, M.; Knoop, G.J. Dissociation constants of some alkanolamines at 293, 303, 318 and 333 K. *J. Chem. Eng. Data* **1990**, *35*, 276–277. [CrossRef]
54. Edwards, T.; Maurer, G.; Newman, J.; Prausnitz, J. Vapor-liquid equilibria in multicomponent aqueous solutions of volatile weak electrolytes. *AIChE J.* **1978**, *24*, 966–976. [CrossRef]
55. Guo, D.; Thee, H.; Tan, C.Y.; Chen, J.; Fei, W.; Kentish, S.; Stevens, G.W.; da Silva, G. Amino Acids as Carbon Capture Solvents: Chemical Kinetics and Mechanism of the Glycine + CO_2 Reaction. *Energy Fuels* **2013**, *27*, 3898–3904. [CrossRef]
56. Littel, R.J.; Versteeg, G.F.; Van Swaaij, W.P.M. Kinetics of CO_2 with primary and secondary amines in aqueous solutions—II. Influence of temperature on zwitterion formation and deprotonation rates. *Chem. Eng. Sci.* **1992**, *47*, 2037–2045. [CrossRef]
57. Xu, S.; Wang, Y.-W.; Otto, F.D.; Mather, A.E. Kinetics of the reaction of carbon dioxide with 2-amino-2-methyl-1-propanol solutions. *Chem. Eng. Sci.* **1996**, *51*, 841–850. [CrossRef]
58. Benamor, A.; Al-Marri, M.J. Reactive Absorption of CO_2 into Aqueous Mixtures of Methyldiethanolamine and Diethanolamine. *Int. J. Chem. Eng. Appl.* **2014**, *5*, 291–297. [CrossRef]